*Remote Sensing for Environmental Monitoring and Change Detection*
*(Proceedings of Symposium HS3007 at IUGG2007, Perugia, July 2007).* IAHS Publ. 316, 2007.

# Estimating evapotranspiration of arid regions using remotely-sensed data

**SEIFELDIN H. ABDALLA[1] & CHRISTOPHER NEALE[2]**

1 *Ministry of Irrigation and Water Resources, Sudan*
seif_eltwaim@yahoo.com

2 *Biological and Irrigation Engineering Dept., Utah State University, Logan, Utah 84322-4105, USA*

**Abstract** Classified airborne high resolution multispectral video imagery (pixel size of 0.16 m) and ground reflectance measurements were used to estimate and map the energy balance terms, namely, net radiation ($R_n$), sensible heat flux ($H$), and ground heat flux ($G$) in a desert environment. The data were gathered during summer 1994, at Goshute valley, Nevada, USA. Energy balance fluxes were measured at 10 sites using Bowen ratio and eddy correlation systems. Ground-based and airborne remotely sensed data were taken at the same time during the experiment. Supervised classification was conducted on each high resolution image of the sites to estimate the proportions of each surface (i.e. playa, organic soils, Greasewood, Sagebrush, and Shadescale). Surface temperature was mapped for each site using airborne thermal imagery (pixel size of 0.30 m) obtained using an infrared thermal scanner. $R_n$ was estimated using the $P/T$ ratio suggested by Jackson (1994) for estimating albedo. $H$ was modelled using vegetation parameters extracted from the multispectral video imagery. The values of $G/R_n$ were exponentially related to the soil adjusted vegetation index (SAVI). Maps of the energy balance fluxes were produced based on the class distribution at each desert site. The good agreement between the observed and estimated surface energy fluxes suggests that maps of surface energy fluxes for sparsely vegetated arid regions could be produced at low cost using airborne sensors and used for input and verification of meso-scale atmospheric and energy balance models.

**Key words** arid; energy balance; remote sensing; video image

## INTRODUCTION

The spatial distribution of energy fluxes strongly affects the atmosphere at the local, regional, and global scales (Bingham *et al*., 1991). Unfortunately, this is not considered by most surface energy balance models, which use point measurement flux data to produce unverified surface energy flux maps for heterogeneous regions (Artan, 1996). One of the major shortcomings of the existing energy flux models is that they are unable to describe the surface temperature and vegetation parameters that strongly affect the energy fluxes in areas with sparse vegetation (Running, 1991). This in turn has a great impact on the accuracy of the outputs of distributed energy balance models; general circulation models (GCM) and regional hydrologic models (Rind *et al*., 1990).

Previous research has shown that some terms in the energy balance equation that depend on surface conditions can be calculated from remotely sensed data (Taconet *et al*., 1986; Kustas *et al*., 1989, 2000; Moran *et al*., 1994; Norman *et al*, 1995). Ground-based meteorological data can be employed to evaluate the other remaining terms of the energy balance equation.

The use of satellite imagery to retrieve surface input components of the energy balance equation in highly heterogeneous natural surfaces is hindered by the low spatial resolution of the satellite sensor (Price, 1982; Taconet *et al*., 1986; Irons & Ranson, 1988; Neale, 1991). However, airborne multispectral video or digital remote sensing offers a viable alternative to resolve the surface heterogeneity since calibrated high resolution spectral imagery can be acquired at different scales. The imagery could be used to quantify surface-related input parameters to the energy balance equations (Abdalla *et al*., 1996, 1997; Neale *et al*., 1996; Chavez *et al*., 2005).

The study addresses the potential of using high resolution multispectral video imagery and ground-based remotely sensed data to quantify surface energy fluxes in a spatially distributed manner over a sparsely vegetated surface in Goshute Valley, Nevada, USA.

## THEORY

In the absence of advection or significant storage of energy by vegetation, the basic equation can be expressed as:

$$R_n = H + \lambda E + G \tag{1}$$

where $R_n$ is net radiation, $H$ is sensible heat flux, $\lambda E$ is latent heat flux, and $G$ is ground or soil heat flux. The sign convention is that the right hand term fluxes are positive when leaving the surface and negative towards the surface. $R_n$ convection is opposite to the other fluxes. All fluxes are in W $m^{-2}$.

The net radiation is obtained from the evaluation of incoming and outgoing shortwave components ($R_S$) and long-wave components ($R_L$). Incoming shortwave radiation ($R_{Sin}$) (0.15–4.0 μm) is the direct and diffuse component from the sun and atmosphere while the outgoing shortwave component ($R_{Sout}$) is reflected by the Earth's surface. The incoming long-wave radiation ($R_{Lin}$) is downward emission by gases in the atmosphere, particularly water vapour and carbon dioxide (>4.0 μm) and outgoing longwave radiation ($R_{Lout}$) is terrestrial radiation emitted by the ground surface to the atmosphere. $R_n$ is then given by:

$$R_n = R_{Sin} + R_{Lin} - R_{Sout} - R_{Lout} \tag{2}$$

The outgoing longwave radiant flux density $R_{Lout}$ can be obtained from remotely measured surface temperatures of soils ($T_s$) and canopy ($T_c$) using a thermal infrared scanner and is given by:

$$R_{Louts} = \varepsilon_s \sigma T_s{**}4 \tag{3}$$

and

$$R_{Loutc} = \varepsilon_c \sigma T_c{**}4 \tag{4}$$

where $R_{Lout}$ and $R_{Lout}$ are the outgoing longwave radiation for the soil and canopy, respectively. $\varepsilon_s$ and $\varepsilon_c$ are emissivity values for soil and canopy measured at the site using the procedure described by Hipps (1989), $\sigma$ is the Stefan-Bolzmann constant ($5.67 \times 10^{-8}$ W $m^{-2}$ $k^4$), $T_s$ and $T_c$ are in Kelvin.

$R_{Sout}$ is surface dependent and controlled by the albedo of the surface. Albedo is the ratio of reflected solar radiation from a surface to that incident upon it. The value

of albedo was estimated for soils and vegetation at the different desert ecosystems using ground radiometry and the $P/T$ ratio suggested by Jackson (1984). The incoming longwave radiation was estimated using Brutsaert (1975). The total incoming short-wave radiation was measured using a calibrated reflectance panel and the $P/T$ ratio.

The soil heat flux ($G$) was estimated using the $G/R_n$ relationship developed by Abdalla *et al*. (1997). $G/R_n$ was related to the soil adjusted vegetation index ($SAVI$) as:

$$G/R_n = 0.302\exp(-0.6025SAVI) \quad (5)$$

where $SAVI$ is given by Huete (1988) as:

$$SAVI = [(NIR - RED)/(NIR + RED + 0.5)] \times 1.5 \quad (6)$$

The sensible heat flux ($H$) was computed using the two layer model developed by Abdalla (1997). The model is based on the concept of separating the soils and plants contributions to the total sensible heat flux ($H$) as:

$$H_T = f_i Hc_i + f_j Hs_j \quad (7)$$

where $f_i$, $f_j$ represent the fractional areas covered by the different types of shrubs and soils, respectively. $Hc_i$ and $Hs_j$ are sensible heat fluxes originated from the different types of shrubs and soils, respectively. For more details regarding the theoretical formulation of the model see Abdalla (1997).

The latent heat flux ($\lambda E$) is the only missing term in the energy balance equation (equation 1). $\lambda E$ was estimated as a residual after spatially estimating the other terms $R_n$, $G$, and $H$ using the high resolution multispectral and thermal airborne imagery.

## METHODOLOGY

### Site description

The field research was conducted at a desert shrub site in Goshute Valley, in eastern Nevada, 3–10 June 1994. The study area is approximately 32 km long and 12 km wide, and has an average elevation of 1700 m. Most of the valley is sparsely vegetated with desert shrubs. The predominant species are: Sagebrush (*Artemisia tridentata*), Greasewood (*Sarcobatus vermiculatus*), Shadescale (*Atriplex confertifolia*). Percentage cover in the study area ranges from 19 to 49%. The soil is silty, calcareous and saline. The vegetated surface of the valley is heterogeneous on both small and large scales. Spacing between the individual shrubs is on the order of a few metres.

### Airborne remote sensing

**Image acquisition** Airborne multispectral video imagery was obtained for each desert ecosystem on DOY 159 and 160, 1994, using the USU video/radiometer remote sensing system described by Neale (1991) and Neale & Crowther (1994). The system consists of three filtered monochrome video, COHU 4810 series, high resolution solid-state CCD cameras. The system acquires imagery in the green (0.55 μm), red (0.65 μm), and near-infrared (0.85 μm) part of the spectrum and includes an EXOTECH 4

band radiometer with Landsat Thematic Mapper bands TM1 (0.45–0.52 μm), TM2 (0.52–0.60 μm), TM3 (0.63–0.69 μm), TM4 (0.76–0.90 μm) and an EVEREST thermal infrared radiometer (8–14 μm). The EXOTECH radiometer has interchangeable field-of-view (FOV) lenses. The FOV of the airborne radiometer was set to 1º and it was mounted in a nadir-viewing position to observe a footprint of 20 × 20 pixels in the centre of the video image. The video lenses have a 16 mm focal distance and the aperture was set at f-11.

It is worth noting that aircraft data were acquired during different flight overpasses at different times and days from different altitudes. Only the imagery of highest resolution (0.16–0.20 m pixels) acquired from 186 m will be used in this study.

**Image processing** The S-VHS video tapes containing the three spectral video bands were viewed to identify the different desert sites using the GPS position information encoded on the red band imagery. The individual band monochrome video images were digitized with a high resolution frame grabber at 8-bit resolution. The digitized video images were corrected for lens vignetting and sensor array non-uniformities using the procedure described by Crowther & Neale (1991) and Neale & Crowther (1994). Imagery were also processed to remove aircraft motion effects and registered into three band images using software described by Neale *et al*. (1994). The resulting images were processed with the Earth Resources Data Analysis System (ERDAS) IMAGINE image processing and GIS software. The images were digitized with a 60% overlap which allowed the three band images to be stitched together to form an image mosaic for each desert ecosystem. To minimize bidirectional effects resulting from having the same scene viewed at different sensor view angles, only the centre portion of each image was used in the mosaic. The stitching process was conducted manually with control points located in the overlap zone of adjacent images.

**Image classification** Supervised signature extraction was conducted for the known classes of vegetation and soils using the ground truth information obtained at each site. The ground truthing was based on: (a) analysis of photographs taken at each site during the same period as the airborne data collection; (b) personal experience gained during the field work period; and (c) bidirectional reflectance measurements of each class using a portable EXOTECH radiometer.

Training samples were selected to identify known classes (e.g. playas, organic soils, Sagebrush, etc.) in order to generate a parametric spectral signature in the three spectral bands. Due to the small scale heterogeneity of the ecosystem, extraction of the signatures was conducted using the supervised seeding technique in ERDAS, which allowed for the location, selection, and generation of representative training sample statistics from the image file to be classified.

The variability within the different individual classes (e.g. due to sun angle or bidirectional effects) were identified and taken into account by training several signatures for the same class. Then spectrally similar signatures were merged to form one signature for the class while statistically separable signatures of the same class were allowed to remain in the pool.

Signature reparability was analysed using the transformed divergence (TD) method suggested by Swain & Davis (1978). This method considers the mean and covariance of the signature in the bands of interest producing lower and upper bounds. The TD interval is between 0 and 2000. The calculated divergence is zero for totally

inseparable signatures and 2000 for perfectly separable signatures. In order to obtain good separation between the spectral classes, a lower bound of 1700 was used.

After creating and evaluating the separable signatures of the different classes for each desert ecosystem, the classification was performed on the entire mosaics using a Maximum Likelihood scheme.

Surface temperatures were mapped using an INFRAMETRICS 760 thermal infrared scanner mounted together with the USU airborne system described above. The 8–14 μm filters were used. The resulting images were corrected for both vertical and horizontal aircraft motion effects and classified into two classes using an unsupervised classification scheme since the two classes were spectrally different (soils and vegetation). Apparent surface temperatures were calculated from the thermal imagery based on the average digital number value of each class and using the calibration bar associated with each image. Apparent temperatures were corrected using soil and vegetation emissivities measured at the experiment site using the procedure described by Hipps (1989). No atmospheric corrections of the temperature values were necessary, since atmospheric effects are generally small on thermal imagery acquired from low altitude flights (Perry & Moran, 1994).

## Ground based measurements

**Remote sensing measurements** Reflectance of the different plant communities and soil types were obtained using an EXOTECH radiometer and a calibrated barium sulphate standard reflectance panel (Jackson *et al*., 1987) with known bi-directional properties. Five measurements were taken from each individual class and then triple readings of the varieties in the same class were also measured (e.g. high, medium, and low Sagebrush). The fifteen measurements were averaged to represent the composite plant or soil spectra for that given class.

During the airborne data collection, a second EXOTECH radiometer was placed overlooking the reflectance panel from nadir, at Bowen Ratio #1 site, to measure incoming irradiance in the same spectral bands. Under clear skies and stable weather conditions, the measurement of partial incoming solar radiation ($R_{sin}$) can be extended over a relatively large area, and applied to the other sites (Asrar, 1989). The ground-based EXOTECH instrument had band pass filters identical to those of the aircraft and panel radiometers (TM bands). All EXOTECH radiometers were cross-calibrated over the panel, on each flight day. Reflectance was calculated using the average of the measurements taken over each class weighted by their time and the corresponding interrelated panel reading at that time. The bidirectional reflectance is given by Neale *et al*. (1989) as:

$$R_c(0, \theta) = L_c / L_p \times R_p(0, \theta) \quad (8)$$

where $R_c(0, \theta)$ is the class bidirectional reflectance, $L_c$ is the class radiance measured with the radiometer (W $m^{-2}$ $SR^{-1}$), $L_p$ is the radiance measured over the panel (W $m^{-2}$ $SR^{-1}$), and $R_p$ $(0, \theta)$ is the bidirectional reflectance of the panel, for a 0° view angle and $\theta$ zenith angle.

**Micrometeorological data** Air temperature, vapour pressure, and the energy balance fluxes were acquired at six sites distributed across the valley at different desert ecosystems using eddy covariance and Bowen ratio systems.

## MAPS OF ENERGY BALANCE FLUXES

Layers of instantaneous net radiation were produced by integrating layers of the different input parameters in the net radiation equation (albedo, emissivity, and surface temperature maps). A map representing the spatial distribution of $R_n$ at Bowen ratio #1 site is shown in Fig. 1.

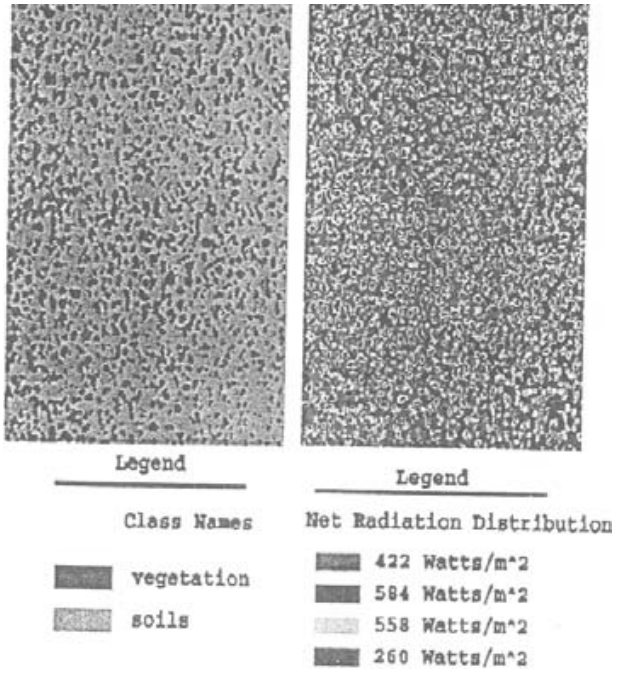


**Fig. 1** Layer of the spatial distribution of $R_n$ for the BR#4 site.

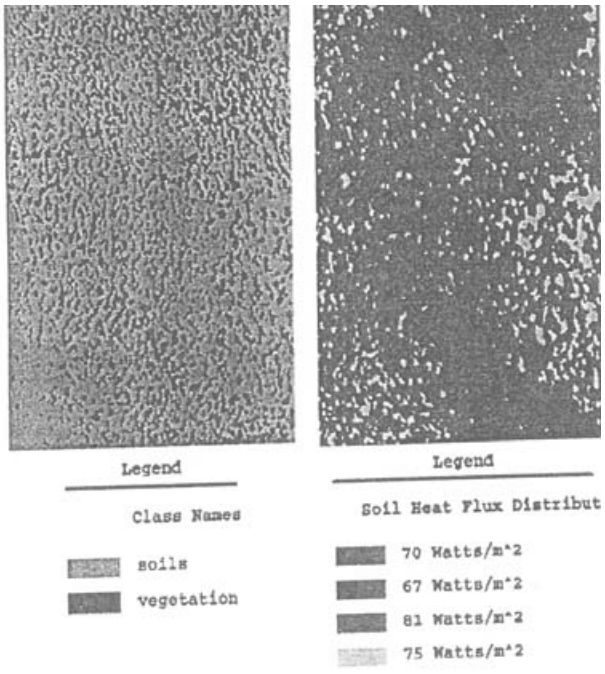


**Fig. 2** Spatial distribution of the soil heat flux at the BR#1 site.

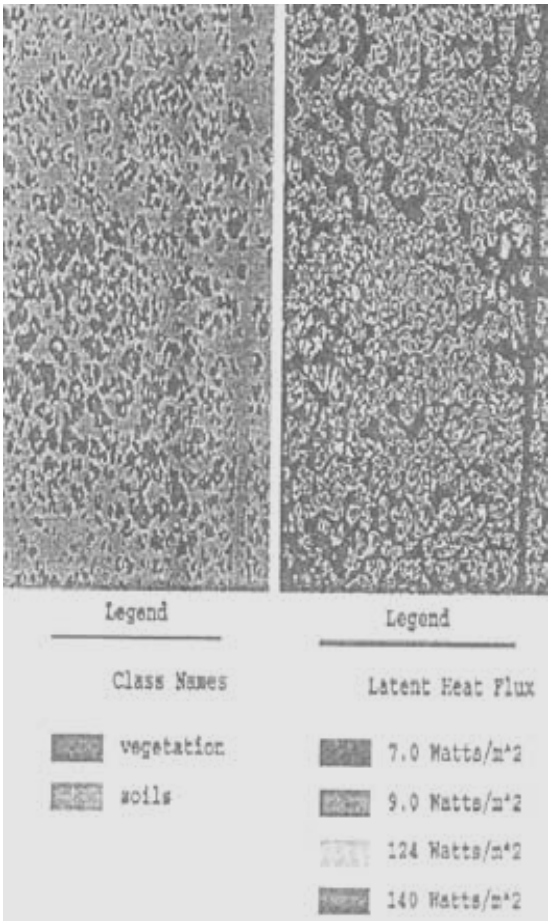


**Fig. 3** A layer of remotely sensed *LE* at the playa.

The spatial distribution of the soil heat flux at the different desert ecosystems was produced using layers of net radiation and SAVI calculated from the remotely sensed data according to equations 5 and 6. Figure 2 shows the spatial distribution of soil heat flux at Bowen ratio #4 site.

Layers of sensible heat flux were produced based on the two-layer model output of the different contributions of plants and soils to the total sensible heat flux in different ecosystems (Abdalla, 1997). The spatial distribution of *H* was estimated using micro-meteorological and remotely sensed inputs. The resulting *H* depends on the spatial distribution of the aerodynamic resistances and the roughness coefficient estimated by Lettau (1969). An example of sensible heat flux distribution at the playa site is given in Fig. 3.

Layers of local scale latent heat flux (pixel size of 0.16 m) were produced using equation (1) and the layers of net radiation, soil heat flux, and sensible heat flux for different desert ecosystems. A map illustrating the spatial distribution of *LE* at the transect 600 site is shown in Fig. 4. The average class-weighted *LE* in each map was verified by comparing it to the *LE* obtained by eddy correlation measurements over each site. In this study, the mean absolute percent difference |MPD| between the mapped and measured LE was 8%. Hence, the error in mapping LE is on the order of uncertainty of conventional ground-based instruments, such as the Bowen ratio method.

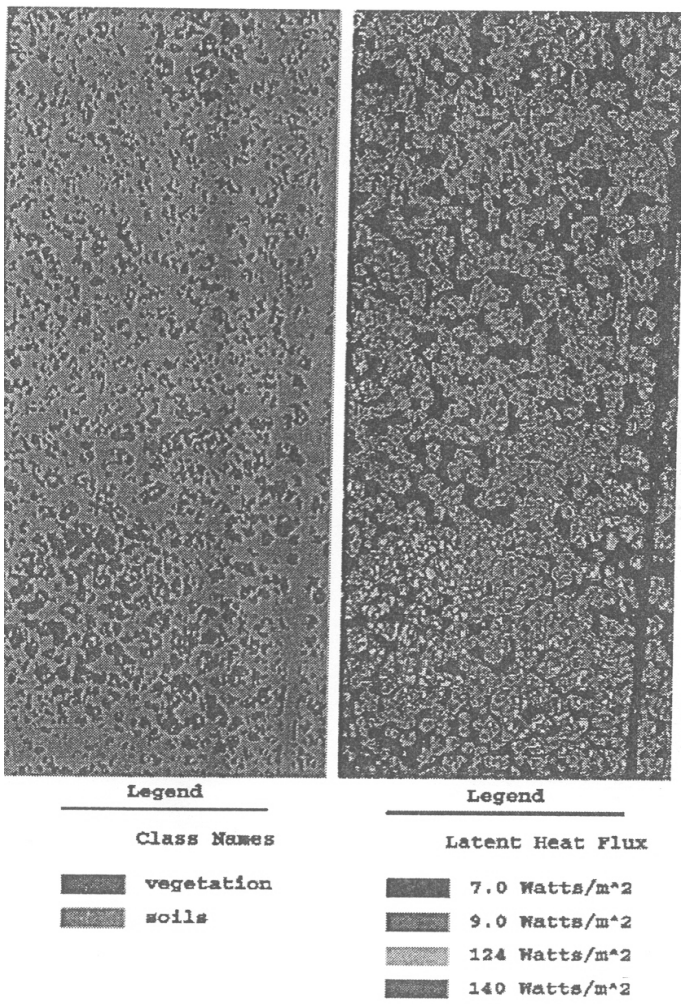


**Fig. 4** A layer of remotely sensed *LE* for Transact-400, DOY 159, 1994 Goshute Valley, Nevada, USA.

## CONCLUSIONS

The good agreement between the measured and mapped energy flux components in sparsely arid ecosystems suggests that local scale high resolution multispectral video imagery can be used to map regional energy balance fluxes.

**Acknowledgments** This research was supported in part by NASA contract NAG-52043 and the Utah Agricultural Experiment Station.

## REFERENCES

Abdalla, S. H. (1997) Surface heat flux estimation for arid regions using remotely sensed data. PhD Dissertation, Utah State Unversity, Logan, Utah, USA.

Abdalla, S. H., Neale, C. M. U., Hipps, L. E. & Malek, E. (1997) Spatial and temporal variation of soil heat flux in sparsely vegetated arid regions. In: *17th Annual American Geophysical Union* (Hydrology Days, Fort Collins, Colorado), 1–12.

Abdalla, S. H., Neale, C. M. U., Malek, E., Hipps L. & Bingham, G. (1996) Estimation of net radiation of sparse vegetation using multispectral video imagery. In *16th Annual American Geophysical Union* (Hydrology Days, Fort Collins, Colorado).

Artan, G. A. (1996) A spatially distributed energy flux model based on remotely sensed and point measured data. PhD Dissertation, Utah State University, Logan, USA.

Asrar, G. (1989) *Theory and Application of Optical Remote Sensing*. John Wiley & Sons, New York, USA.

Bingham, G. E., Neale, C. M. U., Hipps, L. Astling E. & Quattrochi. D. (1991) Mesoscale study of surface heat fluxes and boundary layer processes in a desert region. Utah State University, USA.

Brutsaert, W. (1975) On a derivable formula for long-wave radiation from clear skies. *Water Resour. Res.* **11**, 742–744.

Chávez, J. L., Neale, C. M. U., Hipps, L. E., Prueger, J. H. & Kustas, W. P. (2005) Comparing aircraft-based remotely sensed energy balance fluxes with eddy covariance tower data using heat flux source area functions. *J. Hydromet.* **6**(6), 923–940.

Crowther, B. G. & Neale, C. M. U. (1991) Calibration of multispectral video imagery. In: *Proc. ASAE Symp. Automated Agriculture for the 21st Century* (Chicago, Illinois, December, ASAE).

Hipps, L. E. (1989) The infrared emissivities of soil and *Artemisia tridentata* and subsequent temperature corrections in a shrub-steppe ecosystem. *Remote Sens. Environ.* **27**, 337–342.

Irons, J. R., Ranson, K. J. & Daughtry. C. S. T. (1988) Estimating Big Bluestem albedo from directional reflectance measurements. *Remote Sens. Environ.* **25**, 185–199.

Jackson, R. D. (1984) Total reflected solar radiation calculated from multi-band sensor data. *Agric. For. Met.* **33**, 163–175.

Jackson, R. D., Moran, M. S. Slater, P. N. & Biggar, S. F. (1987) Field calibration of reference reflectance panels. *Remote Sens. Environ.* **22**, 145–158.

Kustas, W. P., Choudhury, B. J., Moran, M. S., Reginato, R. J., Jackson, R. D., Gay, L. W. & Weaver, H. L. (1989a) Determination of sensible heat flux over sparse canopy using thermal infrared data. *Agric. For. Met.* **44**, 197–216.

Kustas, W. P. & Norman, J. M. (2000) A two-source energy balance approach using directional radiometric temperature observations for sparse canopy covered surface, *Agronomy J.* **92**, 847–854.

Lettau, H. (1969) Note on aerodynamic roughness-parameter estimation on the basis of roughness element discription. *J. Appl. Met.* **8**, 828–832.

Moran, M. S., Kustas, W. P., Vidal, A., Stannard, D. I., Blanford, J. H. & Nichols, W. D. (1994) Use of ground-based remotely sensed data for surface energy balance evaluation of a semiarid rangeland. *Water Resour. Res.* **30**(5), 1339–1349.

Neale, C. M. U. (1991) An airborne multispectral video/radiometer remote sensing system for agricultural and environmental monitoring, 293–299. *Proc. Am. Soc. Agric. Engrs Symp.*.

Neale, C. M. U. & Crowther, B. (1994) An airborne multispectral video/radiometer remote sensing system: development and calibration. *Remote Sens. Environ.* **32**(3), 187–194.

Neale, C. M. U., Bausch, W. & Heermann, D. (1989) Development of reflectance based crop coefficients for corn. *Trans Am. Soc. Agric. Engrs* **32**(6),1891–1999.

Neale, C. M. U., Kupier, J., Qui, X. & Tarbet, K. L. (1994) Image enhancement and processing automation routines for digital multispectral video imagery. In *Biennial Workshop on Color Photography and Videography in Resource Monitoring* (Utah State University, Logan, Utah), 29–36.

Neale, C. M. U., Ahmed, R. H., Moran, M. S., Pinter, P. J., Qi, J. & Clarke, T. R. (1996) Estimating seasonal cotton evapotranspiration using canopy reflectance. In: *Int. Conf. on Evapotranspiration and Irrigation Scheduling* (American Society of Agricultural Engineers, San Antonio, Texas), 173–181.

Norman, J. M., Kustas, W. P. & Humes, K. S. (1995) A two-source approach for estimating soil and vegetation energy fluxes in observations of directional radiometric surface temperature. *Agric. For. Met.* **77**, 263–293.

Perry, E. M. & Moran, M. S. (1994) An evaluations for atmospheric corrections of radiometric surface temperatures for a semiarid rangeland watershed. *Water Resour. Res.* **30**, 1261–1269.

Price, J. C. (1982) Estimation of regional scale evapotranspiration through analysis of satellite thermal-infrared data. *IEEE Trans. Geosci. Remote Sens.* **GE-20**, 286–292.

Rind, D., Goldberg, R. Hansen, J.. Rosenzweig, C. & Ruedy. R. (1990) Potential evapotranspiration and the likelihood of future drought. *J. Geophys. Res.* **95**, 9983–10 004.

Running, S. W. (1991) *Computer Simulation of Regional Evapotranspiration by Integrating Landscape Biophysical Attributes with Satellite Data*. Springer-Verlag, New York, USA.

Swain, P. H. & Davis. S. M. (1978) *Remote Sensing: The Quantitative Approach*. McGraw Hill, New York, USA.

Taconet, O., Bernard, R. & Vidal-Madjar, D. (1986) Evapotranspiration over an agricultural region using a surface flux/temperature model based on NOAA-AVHRR data. *J. Clim. Appl. Met.* **25**, 284–307.